Toxicology Letters 207 (2011) 306–313

Contents lists available at SciVerse ScienceDirect

Toxicology Letters

journal homepage: www.elsevier.com/locate/toxlet

Effect of 45 nm silver nanoparticles (AgNPs) upon the smooth muscle of rat trachea: Role of nitric oxide

Carmen González[a,d,*], Samuel Salazar-García[a], Gabriela Palestino[a], Pedro P. Martínez-Cuevas[a], Manuel A. Ramírez-Lee[a], Brenda B. Jurado-Manzano[a], Héctor Rosas-Hernández[a], Noemí Gaytán-Pacheco[b], Guadalupe Martel[b], Ricardo Espinosa-Tanguma[b], Alexandru S. Biris[c], Syed F. Ali[d]

[a] Universidad Autónoma de San Luis Potosí, Facultad de Ciencias Químicas, San Luis Potosi, Mexico
[b] Universidad Autónoma de San Luis Potosí, Facultad de Medicina, San Luis Potosi, Mexico
[c] Nanotechnology Center, University of Arkansas at Little Rock, AR, USA
[d] Neurochemistry Laboratory, Division of Neurotoxicology, National Center for Toxicological Research, US Food and Drug Administration, 3900 NCTR Road, Jefferson, AR, USA

ARTICLE INFO

Article history:
Received 7 February 2011
Received in revised form
22 September 2011
Accepted 23 September 2011
Available online 1 October 2011

Keywords:
Trachea
Silver nanoparticles
Hyper-reactivity
Acetylcholine
NO

ABSTRACT

AgNPs have been used to manufacture nanomaterials with new biophysical properties and functions. However, few experimental approaches have been used to assess their potential toxic or beneficial effects on human health, in association with the size, concentration, and biological target. The aim of this work was to evaluate the effects of the AgNPs on the smooth muscle of rat trachea. A single administration of AgNPs did not modify the smooth muscle tone, but, when the trachea rings were pre-treated with acetylcholine (ACh), AgNPs produced a contractile effect. Simultaneous administration of AgNPs and ACh resulted in a slight increase of smooth muscle contractility induced by ACh. AgNPs pretreatment followed by ACh administration showed that AgNPs exerted an important contraction effect induced by ACh after which muscle tone did not return to the basal level. This effect was associated with an increase in the production of nitric oxide (NO). The contractile response of the AgNPs induced by ACh was completely blocked when the rings were incubated, after the ACh but before the AgNPs administration, with 1400 W (NO blocker). The contractile effect was also abolished by atropine, which suggests that AgNPs alter ACh muscarinic receptor signaling. These data also show that AgNPs modify the contractile action of ACh through NO production and possibly induce hyper-reactivity of tracheal smooth muscle.

1. Introduction

Nanotechnology is a promising field for the generation of new therapies in medicine. Nanoparticles (NPs) are defined as structures with a diameter less than 100 nm and novel physical and chemical properties that differ sharply from the macro forms. While the medical use of AgNPs is growing mainly due to their antimicrobial properties, their respiratory system effects are not well understood (Chen and Schluesener, 2008; Hussain and Schlager, 2009). The hazards associated with human exposure to nanomaterials should be investigated in order to facilitate the risk assessment process (Foldbjerg et al., 2011; Bonner, 2010), and the respiratory system represents the main route of exposure to NPs (Bonner, 2010). Accumulative evidence shows that AgNPs exert controversial effects on the lung and air pathways (Kim et al., 2010; Hussain and Schlager, 2009; Foldbjerg et al., 2011; Sung et al., 2008, 2009).

Studies in a human lung cell line A549 showed that AgNPs induced cytotoxicity and genotoxicity, generating DNA adducts associated with the increase in the cellular reactive oxygen species (ROS). Antioxidant pretreatments prevented those effects, suggesting that AgNPs act as a mediator of ROS-induced genotoxicity (Foldbjerg et al., 2011). Studies *in vivo* of inhaled AgNPs have shown that sub-chronic, 90-day, prolonged exposure produces inhalation toxicity, which affects the liver and lungs (Ji et al., 2007; Sung et al., 2009). Effects in lungs have been previously reported: a decrease in the tidal and minute volumes was observed, as well as inflammatory responses such as mixed inflammatory cell infiltration and chronic alveolar inflammation (Sung et al., 2008). However, the mechanism underlying observed alterations in airway reactivity is complex and not completely understood. Factors such as the release and action of inflammatory cytokines, as well as the signaling molecule (NO) and neurotransmitter (ACh) expression levels

* Corresponding author at: Universidad Autónoma de San Luis Potosí, Av. Manuel Nava Num. 6, Col. Universitaria, Zip Code 78210, Facultad de Ciencias Químicas, San Luis Potosí, México. Tel.: +52 444 8262440x566.
E-mail address: gonzalez.castillocarmen@fcq.uaslp.mx (C. González).

0378-4274/$ – see front matter © 2011 Elsevier Ireland Ltd. All rights reserved.
doi:10.1016/j.toxlet.2011.09.024

are involved (Prado et al., 2006; Nurkiewicz and Porter, 2006; Antošová et al., 2006; Courtois et al., 2008; Español et al., 2010; Huang and Vita, 2006; Ricciardolo, 1997; Ricciardolo et al.,2004).

Nitric oxide (NO) is involved in multiple biological processes, including the release of the inflammatory mediators associated with NPs (Nurkiewicz and Porter, 2006; Courtois et al., 2008). NPs are important factors in the development of pathological changes in the respiratory tract (Courtois et al., 2008) related to host defense, immune regulation, platelet aggregation, neurotransmission, and inflammation (Yamawaki and Iwai, 2006; Brook et al., 2004; Seaton et al., 1995; Liao et al., 1999; Nemmar et al., 2002). NO is synthesized from L-arginine by NO synthases (NOS), which is located in the cells of smooth muscle, epithelium, nerves, endothelium, blood vessels, and inflammatory tissues (Prado et al., 2006; Antošová et al., 2006). The neuronal (nNOS) and endothelial (eNOS) are considered constitutive and are involved in vaso and bronchodilation (Courtois et al., 2008; Prado et al., 2006; Hasaneen et al., 2003). The inducible NOS (iNOS) is stimulated and produces NO in large amounts by many pro-inflammatory cytokines and is expressed in several types of inflammatory tissues (Ricciardolo, 1997; Ricciardolo et al., 2004). It is known that excessive NO produced mainly by iNOS is responsible for the development of many respiratory diseases and their symptoms include bronchial hyper-reactivity (Antošová et al., 2006). ACh, a well-known transmitter of parasympathetic nerve fibers in the airways, is a major regulator of the normal respiratory physiology and one of the strongest constrictors in airway inflammatory diseases (Kummer et al., 2008). In fibroblast cells, activation of muscarinic ACh receptors due to the activation of iNOS can mimic mild inflammatory conditions mediated by an excessive production of NO. This fine-tuned set up of fibroblasts, in turn, can alter the immune system (Español et al., 2010) and is probably involved in hyper-reactivity processes. Based on these observations, the goal of the work presented here was to investigate the role of AgNPs in rat trachea hyper-reactivity and their involvement in the excessive NO production related to an alteration of the ACh signaling pathway.

2. Materials and methods

2.1. Chemicals

AgNPs (45 nm diameter) were purchased from Novacentrix Inc., Austin, TX. Silver bulk materials (<300 nm; BM) and other chemicals were purchased from the Sigma Chemical Company (St. Louis, MO).

2.2. Dispersion of AgNPs in solution

Agglomerate, but relatively homogeneous, NPs dispersions (10 mg/ml stock solutions) were prepared by brief sonication (Cole-Parmer 470 50 W ultrasonic tip processor). AgNPs were dispersed in sterile deionized water. Various final concentrations were prepared in Krebs–Henseleit (KH) physiologic solution for rat trachea smooth muscle rings bioassays (Rosas-Hernández et al., 2009).

2.3. Transmission electron microscopy (TEM) of AgNPs

Physical characterization was performed using a Hitachi H-7600 tungsten-tip transmission electron microscope (TEM), with an accelerating voltage of 120 kV. AgNPs were examined after suspension in water and subsequent deposition onto formvar/carbon-coated TEM grids. The advanced microscopy software for the digital TEM camera was calibrated for size measurements of the NPs. Mean size and SD were calculated from a random field of view, in addition to images that show agglomeration and general morphology, as well as content of another element present with the Ag-45 nm NPs (Rodríguez-Manzo et al., 2007).

2.4. Dynamic light scattering (DLS) of AgNPs

Zeta potential and NP size distribution measurements were realized in a Malvern Zeta potential analyzer at 25 °C, using as dispersant physiological buffer and with a rate count of 40 kcps.

2.5. UV–vis analysis

Absorbance spectra of AgNPs at concentrations of 0.1, 10 and 100 μg/ml dissolved in (a) KH physiologic solution and (b) 10 μM acetylcholine/KH physiologic solution were recorded using a UV–vis Cary 50 spectrophotometer, with 1 cm path way cell. The baseline during the experiment was made using the KH physiologic solution as reference.

2.6. Smooth muscle tone of rat tracheal rings

Adult male Sprague Dawley rats (300–350 g) were sacrificed by an overdose injection of sodium pentobarbital in accordance with animal protocols approved by the Animal Care Committee of the Universidad Autónoma de San Luis Potosí. Experiments were performed as previously described (Algara-Suárez et al., 2007; Rosas-Hernández et al., 2009). Upon sacrifice, the trachea was excised, the epithelium was removed by gently rubbing with a cotton swab, cleansed of adhering tissue, and cut in 3–4 mm wide segments. Individual tracheal rings were suspended from a Radnoti isometric transducer in oxygenated tissue baths containing bicarbonate-buffered Krebs-Henseleit (KH) solution at 37 °C (118 mM NaCl, 4.6 mM KCl, 27.2 mM $NaHCO_3$, 1.2 mM KH_2PO_4, 1.2 mM $MgSO_4$, 1.75 mM $CaCl_2$, 0.03 mM Na_2EDTA and 11.1 mM glucose, 3 μM indomethacin pH 7.4). A passive load of 2 g was applied, and the trachea segments were allowed to equilibrate for 1 h. Smooth muscle of rat tracheal rings was pre-contracted in the presence or absence of 10 μM acetylcholine (ACh), followed by different concentrations of AgNPs (0.1–100 μg/ml). ACh treatment was used as a positive control to invoke smooth muscle contraction. Atropine, an ACh blocker (Kummer et al., 2008), was used as a negative control of contraction, and 1400 W, a specific inhibitor of iNOS (Prado et al., 2006), was used in order to study the role of NO in the contractile effects. The inhibitor 1400 W was administrated after ACh incubation and before the treatments with AgNPs. Real-time data were collected and analyzed using Poliview software (ADI Instruments, Colorado Springs, CO).

2.7. Nitric oxide production

The oxidation products of NO, nitrite (NO_2), and nitrate (NO_3) were determined by the Griess reaction (Kelm and Schrader, 1988; Rosas-Hernández et al., 2009). NO products were determined from tracheal ring samples, collected in the KH solution after treatments were completed. Absorbance was measured using a 540 nm filter (Bio-Rad, Hercules, CA, USA). Assay sensitivity was 1 μM, and the standard curve was produced for NO concentrations ranging from 1 to 200 μM.

2.8. Tissue preparation and iNOS expression

2.8.1. Tissue preparation

Whole trachea were obtained from male rats ($n = 18$) weighing 300–350 g that had been sacrificed with an overdose of sodium pentobarbital (130 mg/kg i.p.) in accordance with the Animal Care Committee of the Universidad Autónoma de San Luis Potosí. Tracheae were placed in KH solution. The strip of smooth muscle was cut and dissected to free adipose and connective tissues, and the epithelium was removed by gently rubbing the lumen with a cotton swab. Six groups, each containing three smooth muscle strips, were made and incubated at 37 °C during 1 h in one of the following treatments: (1) Basal, (2) ACh 10 μM, (3) AgNPs 0.1 μg/ml, (4) AgNPs 100 μg/ml, (5) ACh 10 μM + AgNPs 0.1 μg/ml, (6) ACh 10 μM + AgNPs 10 μg/ml, and (7) ACh 10 μM + AgNPs 100 μg/ml.

2.8.2. Western blot analysis

Once smooth muscle strips were incubated under the various treatments, they were place in RIPA lysis buffer supplemented with protease and phosphatase inhibitor cocktail (Millipore, Concord, MA, USA), cut mechanically, lysed by sonication using an Ultrasonic Homogenizer Omni-Ruptor at 20 power out (OMNI International Inc., Marietta, Georgia, USA), and incubated for 30 min on ice. Lysates were centrifuged at 10,000 × *g* for 10 min, and supernatants were recovered. The total protein concentration was quantified by the micro BCA protein assay (Sigma–Aldrich, St. Louis, MO) using a UV spectrophotometer (Bio-Rad Laboratories, Inc., Hercules, CA) at 562 nm. 40–60 μg of total protein were mixed with Laemmli 2× buffer and heated at 95.0 °C for 10 min. Total protein was subjected to 105 SDS-PAGE and electrophoretically transferred to 0.2 μm PVDF membranes (Bio-Rad laboratories, Inc. Hercules, CA). Membranes were blocked with 5% nonfat dry milk in Tris-buffered saline (pH 7.6) containing 0.1% Tween (TBST) and probed overnight at 4 °C with goat polyclonal antibody anti-iNOS Dil. 1:200 (Santa Cruz Biotechnology, Inc., Santa Cruz, CA). In addition, all membranes were probed with antibody directed against GAPDH as a control protein. After washing with TBST, the membranes were incubated with donkey anti-goat polyclonal HRP-conjugated Ab (1:5000) in TBST + 5% nonfat dry milk during 1 h 30 min. After subsequent washes, bands were visualized by chemiluminescence (Pierce, Rockford, IL) followed by autoradiography.

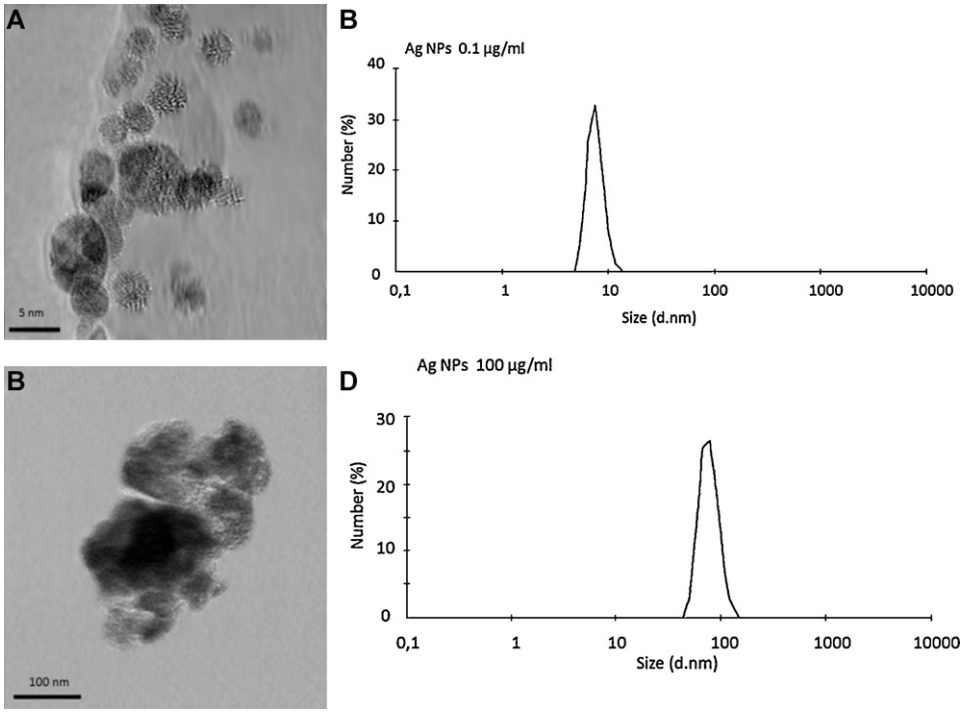

Fig. 1. TEM micrographs showing the AgNPs dispersed in KH buffer solution at (A) 0.1 μg/ml, (B) 100 μg/ml and the correspondent size distribution, (C) 0.1 μg/ml, and (D) 100 μg/ml.

2.9. Data analysis

Datas were expressed as a mean ± SEM of three independent experiments; they were subjected to a statistical analysis by one-way ANOVA followed by Dunnett test for multiple comparisons. Values of $p < 0.05$ were considered significant.

3. Results

3.1. AgNPs characterization

3.1.1. TEM analysis of Ag-45 nm NPs

A study of the Ag-45 nm NPs dispersed in KH physiologic solution at 100 and 0.1 μg/ml was performed by transmission electron microscopy (TEM). Analysis of the micrographs showed an AgNPs size distribution ranging from 4 to 90 nm (Fig. 1B and D). Through this analysis, we found that, at the highest concentration, the Ag NPs formed agglomerates (Fig. 1C). On the other hand, when the Ag NPs were examined at the lowest concentration, well-defined spherical NPs with diameters around 4 nm were observed (Fig. 1A and B).

3.1.2. Dynamic light scattering (DLS) studies

The AgNPs dispersed in KH physiologic solution at 100, 10, and 0.1 μg/ml were analyzed by DLS. The zeta potential values found for each concentration were, respectively, as follows: −4.83 ± 4.86, −29.3 ± 5.39, and −26.7 ± 6.05 mV. These results confirm the fact that at higher concentrations there is instability of the Ag colloidal system, which may lead to the formation of the Ag agglomerates. The NPs average diameter was confirmed recording the size distribution profile. The results evidenced a NP mean diameter of 79 nm ± 16 for the 100 μg/ml solution, while, for the 10 and 0.1 μg/ml solutions, the NPs' mean diameter was found to be 29 nm ± 5.3 and 7.6 nm ± 1.3, respectively. The histograms are shown in Fig. 1B and D. These findings are in agreement with our previously published results (Rosas-Hernández et al., 2009).

3.2. AgNPs by themselves do not modify the basal smooth muscle tone of rat trachea, but their administration after treatment with ACh induces contraction

Cumulative concentrations of AgNPs, by themselves, did not modify the basal smooth muscle tone of the rat trachea rings (Fig. 2A). However, AgNPs induced transient contraction when administrated after the treatment with 10 μM ACh (Fig. 2B). The AgNPs 0.1 μg/ml, induced 66.66% of the transient contraction in comparison with the maximum contraction induced by ACh (100%). AgNP concentrations of 1, 10, and100 μg/ml stimulated 36, 33, and 33% of transient contraction, respectively, in comparison with ACh (Fig. 2C).

3.3. The administration order of AgNPs modifies the contractile effect induced by ACh

The concomitant administration of unique doses of AgNPs, 0.1 or 100 μg/ml, and ACh induced a transient contraction in comparison to ACh administrated alone as a positive control (Fig. 3E). Administration of 0.1 μg/ml (Fig. 3A) produced a more robust response than 100 μg/ml of these AgNPs (Fig. 3B) in the presence of 10 μM ACh. On the other hand, when the AgNPs (0.1 or 100 μg/ml) were administrated prior to ACh, the NPs, alone, did not modify the basal muscle tone (Fig. 3C and D). However, AgNPs potentiated twice the maximum contractile effect induced by ACh when administrated in the presence of 0.1 μg/ml (Fig. 3C), and around 1.5 times at 100 μg/ml (Fig. 3D) compared to the maximum contractile effect induced by the ACh control (Fig. 3E and F). Moreover, after several administrations, the relaxation phase of muscle tone did not return to the basal levels, maintaining a constant and permanent contractile effect, at least for the duration of the experiment (Fig. 3B–D).

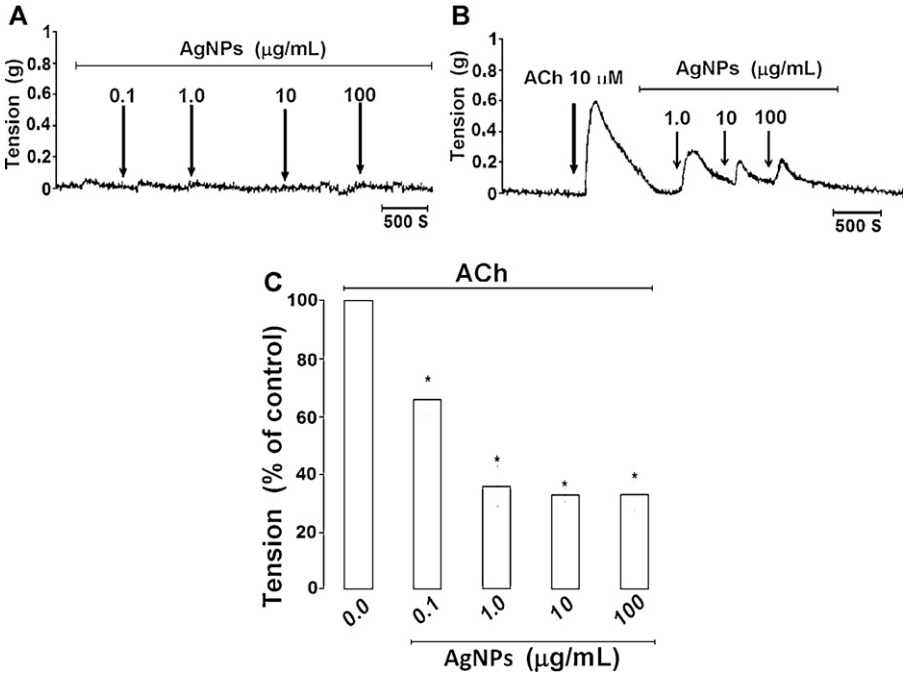

Fig. 2. AgNPs do not modify the basal smooth muscle tone of rat trachea, but their administration in the presence of ACh induces contraction. The figure shows a representative record. The tension in grams was taken as an index of smooth muscle tone of rat trachea and was recorded in the isolated rat tracheal rings. The trachea was treated with increasing concentrations of AgNPs (A) without ACh, (B) contracted by exposure to 10 μM ACh, and (C) graphs that represent the effect in % of contraction with ACh in the presence of increasing concentrations of AgNPs. Results are representative of three independent experiments. Values represent the mean ± SEM; *, $p < 0.05$ vs. control.

3.4. Treatments with AgNPs in the presence of repetitive administrations of ACh and incubations with BMs do not modify the transient contractile effect and, therefore, validate the specificity of the contractile effects induced by AgNPs

In order to validate the specificity of these contractile effects and the viability of the tracheal rings, we performed several treatments that included two repetitive administrations of unique concentrations of ACh. ACh exerted the same transient contraction, in the same magnitude, and returned to basal levels (Fig. 4A). Because the ACh-induced transient contraction is due to the interaction with muscarinic receptors (Kummer et al., 2008), we incubated the tracheal rings in the presence of atropine, 5 μg/ml, which abolished the transient contraction induced by ACh (Fig. 4B). In addition, we confirmed that the actions induced by AgNPs in the presence of ACh were specific, due to the absence of transient contractile effects in the presence of bulk material concentration 0.1 or 100 μg/ml (Fig. 4C and D).

3.5. The ACh incubation following the AgNPs treatments induces excessive NO production in the physiologic solution containing the smooth muscle rat trachea

In order to evaluate the possible mediator involved in the AgNPs actions, we decided to evaluate the NO production, which plays an important role in airway inflammation and hyperactivity, through bronchio-constriction (Antošová et al., 2006; Nurkiewicz and Porter, 2006; Courtois et al., 2008).

NO levels, determined by NO_2/NO_3, were not detected in the initial conditions, nor in the presence of ACh or AgNPs (0.1 or 100 μg/ml). However, the pre-treatment with ACh followed by AgNPs induced a significant increase in NO production in comparison with controls (Fig. 5). This suggests an important role for NO in the contractile properties of AgNPs.

3.6. The AgNPs in the presence of ACh activate iNOS isoform to produce an excessive NO and stimulate the transient tracheal smooth muscle contractility

With the aim to investigate the NOS isoform involved in the transient contractile actions induced by AgNPs in the presence of ACh, (Fig. 6A and B), we pretreated the tracheal rings with L-NAME, an inhibitor of all of the NOS isoforms (Prado et al., 2006). We observed that L-NAME blocked the actions induced by AgNPs in the presence of ACh (Fig. 6C and D). We subsequently used a specific iNOS inhibitor, 1400 W (Prado et al., 2006), that completely blocked the contractile actions induced by AgNPs after administration of ACh (Fig. 6E and F). Moreover, we confirmed the expression of iNOS in the smooth muscle of rat trachea, observing that only the increasing concentrations of AgNPs in the presence of ACh stimulated the iNOS expression, but not the treatment in presence of the AgNPs, alone (without ACh) (Fig. 7). These data indicate that NO is involved in the contraction induced by AgNPs in the presence of ACh due to the activation of iNOS.

3.7. The effects induced by AgNPs-NO dependent on the presence of ACh are blocked by atropine

To examine the possible mechanism of action exerted by the AgNPs in the presence of ACh, we pre-contracted the tracheal rings in the presence of ACh, followed by atropine. Afterward, tracheal rings were incubated in the presence of AgNPs. We observed that the transient contractile effect induced by the AgNPs (Fig. 8A) was completely blocked by atropine (Fig. 8B). Moreover, the treatment with atropine in the presence of ACh and AgNPs did not produce NO in the physiologic solution that contained the tracheal rings under this treatment, compared with ACh plus AgNPs (Fig. 8C). These data suggests that the transient contraction induced by AgNPs interferes with the ACh signaling pathway coupled with iNOS and results in production of NO.

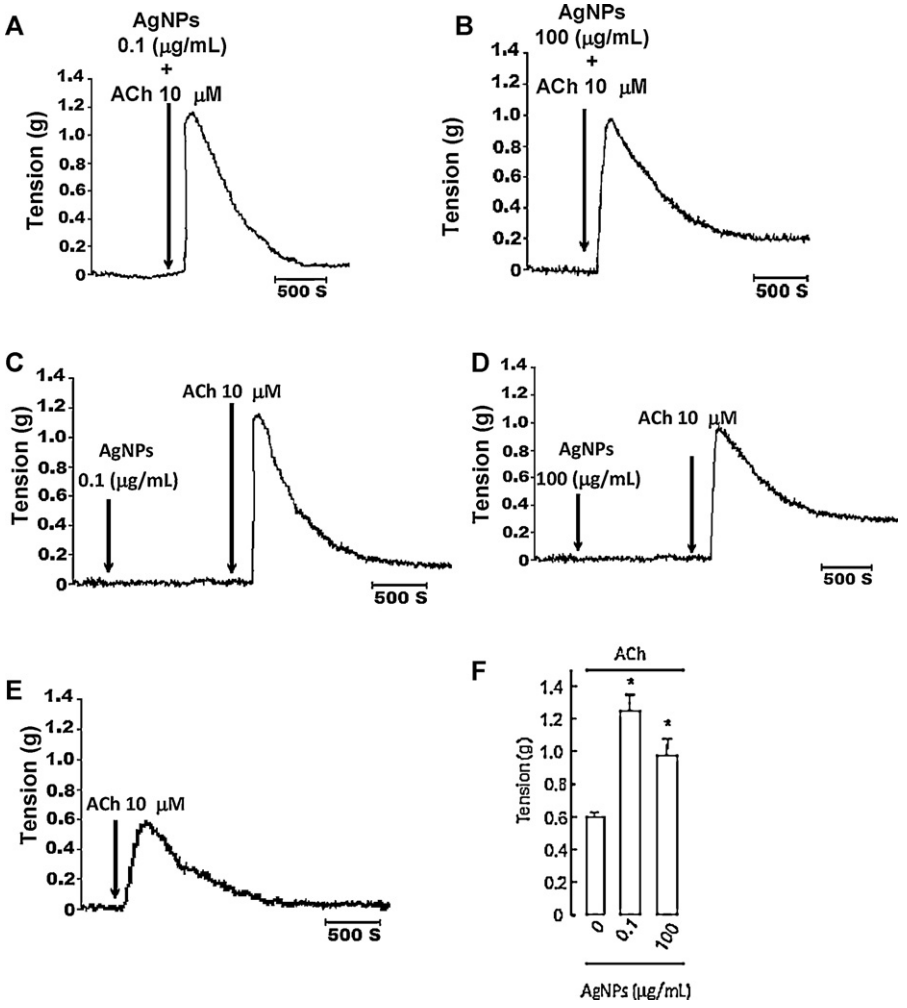

Fig. 3. The administration regimen of AgNPs modifies the contractile effect induced by ACh. The figure shows a representative record. The tension in grams was taken as an index of smooth muscle tone of rat trachea and was recorded in the isolated rat tracheal rings. The trachea was treated in the presence of concomitant administration of ACh and either (A) 0.1 μg/ml AgNPs or (B) 100 μg/ml AgNPs, or when the trachea was treated with a prior administration of either (C) 0.1 μg/ml AgNPs or (D) 100 μg/ml AgNPs followed ACh administration. (E) Record of concentrations in the presence of ACh (positive control). (F) Maximum tension (g) from trace recordings in response to ACh and AgNPs obtained as indicated above from three independent experiments. Values represent the mean ± SEM; $^{*}p < 0.05$ vs. control.

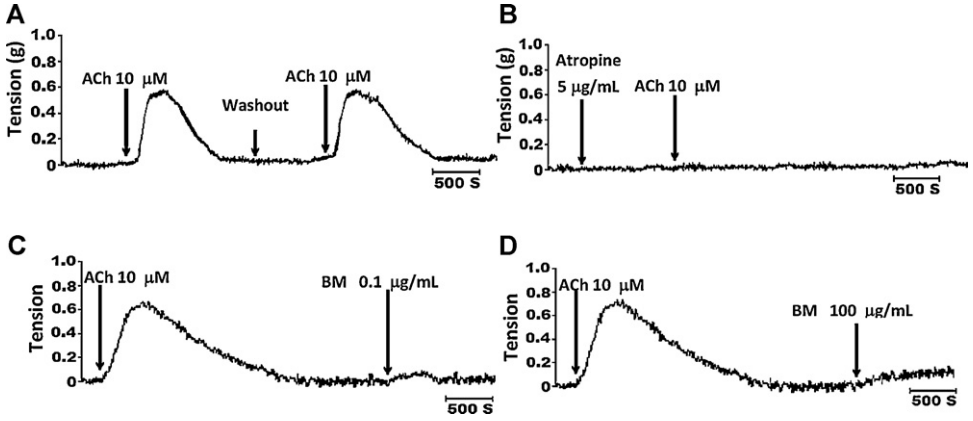

Fig. 4. Repetitive administration of ACh and incubations with BMs do not modify the ACh transient contractile effect, thus validating the specificity of the contractile effects induced by AgNPs. The figure shows a representative record. The tension in grams was taken as an index of the smooth muscle tone of rat trachea and was recorded in the isolated rat tracheal rings. The trachea was (A) treated with 10 μM ACh before and after a washout; (B) pretreated with atropine 5 μg/ml, followed by ACh 10 μM; (C) pretreated with ACh 10 μM, followed BM, 0.1 μg/ml; or (D) pretreated with ACh 10 μM, followed BM,100 μg/ml. Results are representative of three independent experiments.

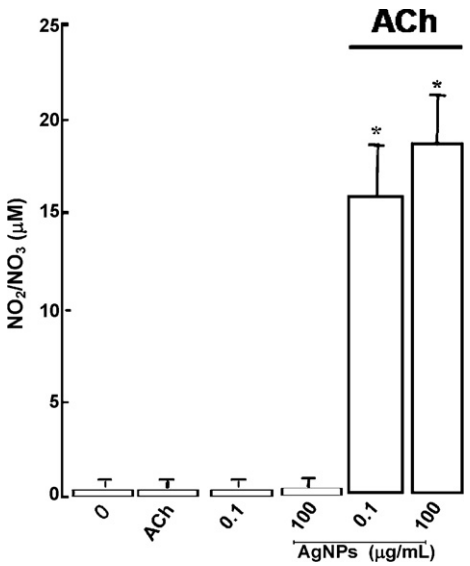

Fig. 5. Exposure to ACh and AgNPs induce an excessive NO production in the physiologic solution that contains the rat tracheal rings. The production of NO was measured by accumulation of nitrites/nitrates in the physiological solution, in the presence of the respective treatments, basal or zero (absence of any treatment), 10 μM ACh, 0.1 μg/ml AgNPs, 100 μg/ml AgNPs, 0.1 or 100 μg/ml ACh + AgNPs. The optical density was measured to 490 nm. Values represent the mean ± SEM; $^*p < 0.05$ vs. control.

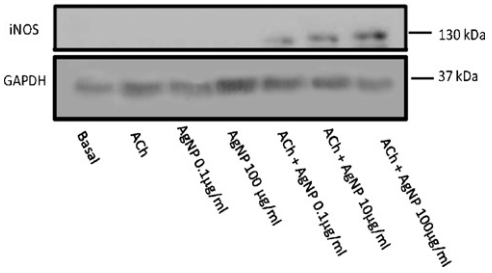

Fig. 7. AgNPs in the presence of ACh induces iNOS expression in the rat tracheal smooth muscle. The smooth muscle stripes were incubated in the presence or absence of various concentrations (0.1–100 μg/ml) of AgNPs and in the presence or absence of ACh 10 μM for 1 h. Tissue lysates were separated by electrophoresis and transferred to membranes followed by immunoblotting with antibodies directed against iNOS and GAPDH as control. Results are representative of three independent experiments.

3.8. Addition of ACh produces an enhancement of the AgNPs plasmon absorption band

The AgNPs exhibit optical properties in the UV/Vis spectrum that are due to a phenomenon known as the surface plasmon absorption band (SPAB). This phenomenon is produced by the oscillations in conduction electrons on the surface of the NPs as a consequence of the incident electric field light, which produces the absorption of electromagnetic radiation. The wavelength of the plasmon absorption maximum (PAM) and its intensity depend on the NPs' size and

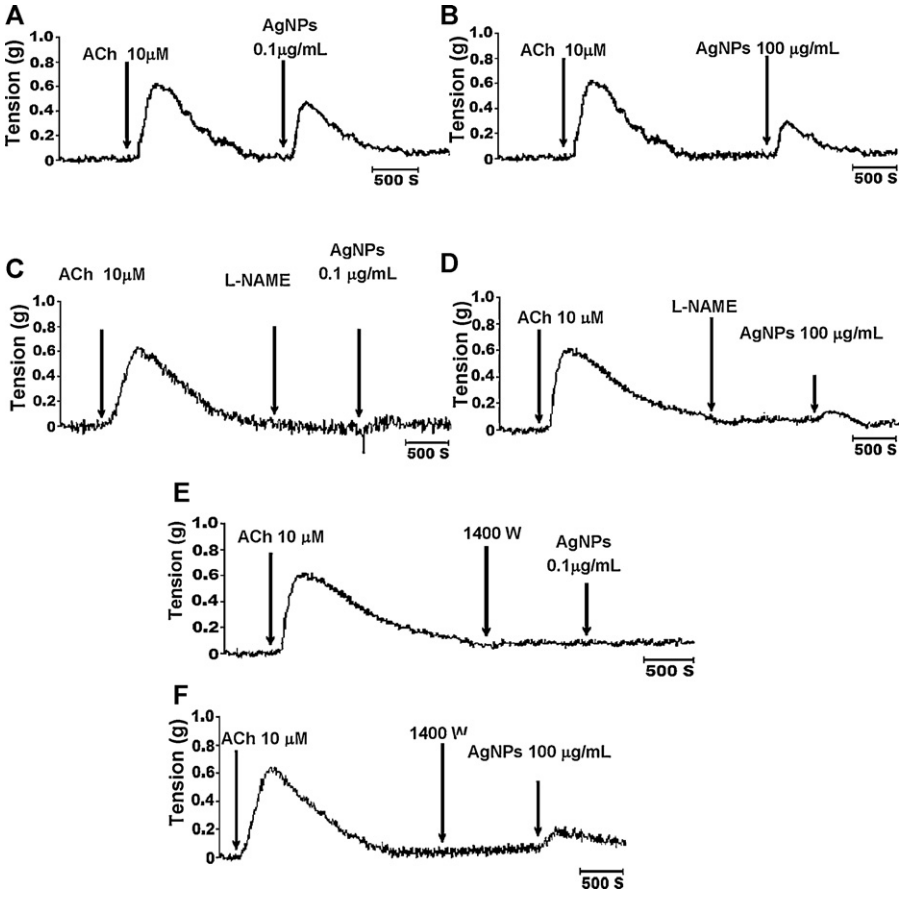

Fig. 6. The contractile effect induced by AgNPs in the presence of ACh depends on the iNOS activity. The figure shows a representative record. The tension in grams was taken as an index of smooth muscle tone of the rat trachea and was recorded in isolated rat tracheal rings. The trachea was treated in the presence of ACh followed by exposure to (A) AgNPs at 0.1 μg/ml, as control of transient contraction with AgNPs; (B) AgNPs at 100 μg/ml, as control of transient contraction; (C) L-NAME 0.5 mM, and exposure to AgNPs at 0.1 μg/ml; (D) L-NAME 0.5 mM, and exposure to AgNPs at 100 μg/ml; E) 1400 W, 0.1 μg/ml, and exposure to AgNPs 0.1 μg/ml; F) 1400 W, 0.1 μg/ml, and exposure to AgNPs at 100 μg/ml. Results are representative of three independent experiments.

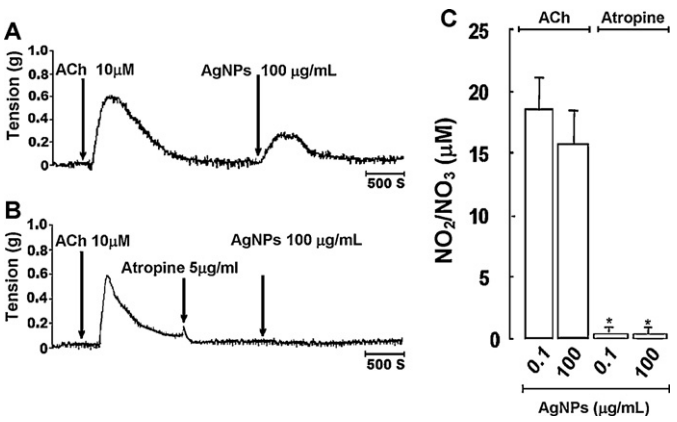

Fig. 8. The contractile effects induced by AgNPs-NO in the presence of ACh are blocked by atropine. The figure shows a representative record. The tension in grams was taken as an index of smooth muscle tone of rat trachea and was recorded in the isolated rat tracheal rings. The trachea was treated in the presence of ACh 10 μM followed by the administration of (A) AgNPs at 100 μg/ml, as control of transient contraction with AgNPs; (B) 5 μg/ml atropine and exposure to AgNPs at 100 μg/ml. The production of NO was measured by the accumulation of nitrites/nitrates in the physiological solution, in the presence and absence of two concentrations of AgNPs, (C) 0.1 or 100 μg/ml, and in the presence of ACh, and ACh/atropine. The optical density was measured to 490 nm. Values represent the mean ± SEM; $^{*}p < 0.05$ vs. control.

shape, as well as the surrounding dielectric medium, coupling of the colloids and adsorbed solutes (Slistan-Grijalva et al., 2005). Thus, any change on the PAM can be used to monitor local changes on the AgNPs surface. We recorded the UV/Vis spectra of AgNPs suspended in different media (Fig. 9): (1) KH physiological buffer and (2) ACh/KH buffer at 10 and 100 μg/ml AgNPs concentration. To have a suitable reference, the spectra of ACh in KH physiological buffer were also taken. The results show that the ACh do not have absorption in the studied UV/Vis spectral region (250–600 nm). Conversely, the AgNPs suspended in KH at 100 μg/ml presented a well-defined peak centered at 394 nm, characteristic of spherical AgNP with diameters in the range of 1–50 nm (Creighton et al., 1979) which confirms the results we obtained by DLS and TEM. No signal was found at the 10.0 μg/ml concentration, possibly due to the low AgNP concentration and limitations on the spectrometer's resolution. However, when ACs were added to the AgNPs suspensions, we observed an important change in the UV/Vis spectra. The PAM absorption intensity at 100.0 μg/ml concentration considerably increases; furthermore, the SPAB that was not seen at 10 μg/ml

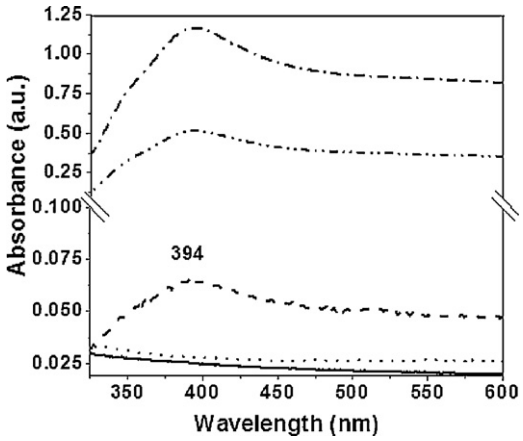

Fig. 9. UV/Vis absorption spectra of ACh suggest interactions with AgNPs. Acetylcholine (10 μM) in KH physiological solution (···) and AgNPs suspended in KH physiological buffer at 10 μg/ml (—) and 100 μg/ml (– · –). AgNPs dispersed in acetylcholine/KH solution at 10 μg/ml (- - -) and 100 μg/ml (– · · –).

concentration in the KH medium, is now easily observed. Since theoretical calculations indicate that the PAM of AgNPs increases with the refractive index of the surrounding medium (Slistan-Grijalva et al., 2005), we may attribute this change to adsorbed ACs at the AgNPs' interface. This hypothesis is supported also taking into account that the refractive index of buffered solutions is lower than that of the biological molecules; therefore, the addition of ACs could affect the refractive index of the medium surrounding the particle, producing the enhancement of its optical properties.

4. Discussion

The present work shows that AgNPs in rat trachea increase the contractile effects induced by ACh, presenting a model for study of the airway hyper-reactivity associated with inflammatory processes. The tracheal smooth muscle contraction induced by AgNPs, in the presence of ACh, promotes the transient contraction in cumulative increasing concentrations. This effect was consistent, in function of the different kinds of administration orders that involve, the concomitant administration of ACh and AgNPs, AgNPs following ACh administration, or ACh followed by AgNPs. The absence of contraction in the presence of AgNPs indicates that the exposure to and action of a contractile stimulator is necessary in order to induce the contractile transient effects by AgNPs. It appears that ACh is essential for the activation receptors and their specific signaling pathways.

In order to evaluate, dissect, and characterize specific effects, mediators, and the possible mechanism of action associated with the AgNPs in the trachea, we applied one type of AgNPs administration. In this regard, the AgNPs administration followed the ACh exposure. We observed that the low NPs concentration was more sensitive to the contractile effects induced by ACh compared to the higher concentration. These actions agree with previous studies (Sung et al., 2008) where the prolonged AgNP inhalation exposure in rats induced lung functional changes, along with inflammation, at much lower concentrations (Sung et al., 2008, 2009). Moreover, the bulk materials did not exert contractile effects. These actions could be related to the aggregation property exhibited by the NPs (Hussain and Schlager, 2009). It is possible that the NPs aggregation due to higher concentration could attenuate their contracted effects. Due to this, we propose a possible interaction between AgNPs and ACh based on the completely blocked contraction, induced by low and high concentrations of AgNPs, as well as with atropine.

It is known that, under normal physiological conditions, the ACh muscarinic receptors coupled to Gq proteins, activate PLC and induce the release of IP_3 which, in turn, stimulates the release of calcium from the sarcoplasmic reticulum (Exton, 1996; Eglen, 2006). However, during inflammatory processes, an alternative mechanism is involved (Español et al., 2010). In fibroblasts, charbacole, a muscarinic agonist, in the presence of bacterial lipopolysaccharides (LPS) and cytokines, such as interferon gamma (IFN γ), activates the muscarinic ACh receptor. This action may mimic inflammatory conditions via iNOS expression and consequently could generate large amounts of NO. ACh receptors can mimic the inflammatory conditions in fibroblasts, establishing a fine-tuned system that could alter the immune system (Español et al., 2010).

Concurrently, NO is an important endogenous mediator involved in many biological functions under physiological and pathological conditions. The inducible NOS (iNOS) is stimulated by many pro-inflammatory cytokines and is expressed in several types of inflammatory cells (Ricciardolo, 1997). Many studies show that high levels of NO play an important role in the regulation of physiological pulmonary function, as well as in the respiratory diseases associated with hyper-activity. Changes in airway smooth muscle

tone and the response to different mediators, including NPs and other ultrafine particles (Courtois et al., 2008), provide evidence of abnormal production of NO in the airways (Antošová et al., 2006).

In conclusion, our work clearly shows that AgNPs could sensitize the trachea prior to the contractile effects of ACh. One possibility is that the NPs interact with the ACh muscarinic receptor that, in turn, stimulates the iNOS activity and the consequent large production of NO. These actions could permanently activate the PLC activity, production of IP_3, and the release of intracellular calcium from sarcoplasmic reticulum or induce the entrance of extracellular calcium. In this experimental model of isolated tracheal smooth muscle, it may be possible that iNOS activity produced NO contractile effects, immediately or in minutes, after the administration of AgNPs in the presence of ACh. It has been shown that, in the airways, NO production takes place due to continuous expression of iNOS in healthy individuals, and this enzyme appears to have a crucial role in defending the airways against infection (Guo et al., 1995). However, in a pathological situation, its presence could impair the activity and regulation of this enzyme, promoting bronchial hyper-reactivity. These data give more information about the toxic effect of AgNPs in the airways and could represent a model to study inflammatory processes linked to airway hyper-reactivity. This research opens new avenues in the study of the mechanism of AgNPs action in specific airway regions and the effects of their interaction with other contractile stimulators.

Conflict of interest statement

None

Acknowledgements

We want to thank Ms. Salma Jiménez Badillo for technical assistance. The editorial assistance of Dr. Marinelle Ringer is also acknowledged. This work was supported by the National Council of Science and Technology of Mexico Grant 105056 and Integral Program for Institutional Support Grants C10-PIFI-09-07.36 and C10-FAI-05-15.42.

References

Algara-Suárez, P., Romero-Méndez, C., Chrones, T., et al., 2007. Functional coupling between the Na/Ca exchanger and nonselective cation channels during histamine stimulation in guinea pig tracheal smooth muscle. Am. J. Physiol. Lung Cell Mol. Physiol. 293 (1), L191–L198.

Antošová, M., Strapková, A., Nosál'ová, G., et al., 2006. Effect of nitric oxide synthases inhibitors on exogenous irritant-induced bronchial hyper-reactivity in guinea pigs. Gen. Physiol. Biophys. 25 (2), 137–147.

Bonner, J.C., 2010. Nanoparticles as a potential cause of pleural and interstitial lung disease. Proc. Am. Thorax Soc. 7 (2), 138–141.

Brook, R.D., Franklin, B., Casio, W., et al., 2004. Air pollution and cardiovascular disease: a statement for health-care professionals from the expert panel on population and prevention science of the American Heart Association. Circulation 109, 2655–2671.

Chen, X., Schluesener, H.J., 2008. Nanosilver: a nanoproduct in medical application. Toxicol. Lett. 176 (1), 1–12.

Courtois, A., Andujar, P., Ladeiro, Y., et al., 2008. Impairment of NO-dependent relaxation in intralobular pulmonary arteries: comparison of urban particulate matter and manufactured nanoparticles. Environ. Health Perspect. 116 (10), 1294–1299.

Creighton, J.A., Blatchford, C.G., Albrecht, M.G., 1979. Plasma resonance enhancement of Raman scattering by pyridine adsorbed on silver or gold sol particles of size comparable to the excitation wavelength. J. Chem. Soc., Faraday Trans. 2 75, 790–798.

Eglen, R.M., 2006. Muscarinic receptor subtypes in neuronal and non-neuronal cholinergic function. Auton. Autacoid Pharmacol. 26 (3), 219–233.

Español, A.J., Goren, N., Ribeiro, M.L., et al., 2010. Nitric oxide synthase I and cyclooxigenase-2 enzymes are targets of muscarinic activation in normal and inflamed NIH3T3 cells. Inflamm. Res. 59 (3), 227–238.

Exton, J.H., 1996. Regulation of phosphoinositide phospholipases by hormones, neurotransmitters, and other agonists linked to G proteins. Annu. Rev. Pharmacol. Toxicol. 36, 481–509.

Foldbjerg, R., Dang, D.A., Autrup, H., 2011. Cytotoxicity and genotoxicity of silver nanoparticles in the human cancer cell line, A549. Arch. Toxicol. 85 (7), 743–750.

Guo, F.H., Raeve, H.R., Rice, T.W., et al., 1995. Continuous nitric oxide synthesis by inducible nitric oxide synthase in normal airway epithelium *in vivo*. Proc. Natl. Acad. Sci. U.S.A. 92 (17), 7809–7813.

Hasaneen, N.A., Foda, H.D., Said, S.I., 2003. Nitric oxide and vasoactive intestinal peptide as co-transmitters of airway smooth-muscle relaxation: analysis in neuronal nitric oxide synthase knockout mice. Chest 124 (3), 1067–1072.

Huang, A.L., Vita, J.A., 2006. Effects of systemic inflammation on endothelium-dependent vasodilation. Trends Cardiovascular Med. 16, 15–20.

Hussain, S.M., Schlager, J., 2009. Safety evaluation of silver nanoparticles: inhalation model for chronic exposure. Toxicol. Sci. 108 (2), 223–224.

Ji, J.H., Jung, J.H., Kim, S.S., et al., 2007. Twenty-eight-day inhalation toxicity study of silver nanoparticles in Sprague-Dawley rats. Inhal. Toxicol. 19 (10), 857–871.

Kelm, M., Schrader, J., 1988. Nitric oxide release from the isolated guinea pig heart. Eur. J. Pharmacol. 155 (3), 317–321.

Kim, Y.S., Song, M.Y., Park, J.D., et al., 2010. Subchronic oral toxicity of silver nanoparticles. Particle Fibre Toxicol. 7, 20.

Kummer, W., Lips, K.S., Pfeil, U., 2008. The epithelial cholinergic system of the airways. Histochem. Cell Biol. 130 (2), 219–234.

Liao, D., Creason, J., Shy, C., et al., 1999. Daily variation of particulate air pollution and poor cardiac autonomic control in the elderly. Environ. Health Perspect. 107 (7), 521–525.

Nemmar, A., Hoet, P.H., Vanquickenborne, B., et al., 2002. Passage of inhaled particles into the blood circulation in humans. Circulation 105 (4), 411–414.

Nurkiewicz, T.R., Porter, D.W., Berger, M., et al., 2006. Systemic microvascular dysfunction and inflammation after pulmonary particulate matter exposure. Environ. Health Perspect. 114 (3), 412–419.

Prado, C.M., Leick-Maldonado, E.A., Yano, L., et al., 2006. Effects of nitric oxide synthases in chronic allergic airway inflammation and remodeling. Am. J. Respir. Cell Mol. Biol. 35 (4), 457–464.

Ricciardolo, F.L., Maria, D.G.U., Mistretta, A., 1997. Impairment of bronchoprotection by nitric oxide in severe asthma. Lancet 350 (9087), 1297–1298.

Ricciardolo, F.L.M., Sterk, P.J., Gaston, B., et al., 2004. Nitric oxide in health and disease of the respiratory system. Physiol. Rev. 84 (3), 731–765.

Rodríguez-Manzo, J.A., Terrones, M., Terrones, H., et al., 2007. *In situ* nucleation of carbon nanotubes by the injection of carbon atoms into metal particles. Nat. Nanotechnol. 2 (5), 307–311.

Rosas-Hernández, H., Jiménez-Badillo, S., Martínez-Cuevas, P.P., et al., 2009. Effects of silver nanoparticles (Ag-45 nm) upon coronary endothelial cells and isolated aortic rings. Toxicol. Lett. 191 (2–3), 305–313.

Seaton, A., MacNee, W., Donaldson, K., et al., 1995. Particulate air pollution and acute health effects. Lancet 345, 176–178, 8943.

Slistan-Grijalva, A., Herrera-Urbina, R., Rivas-Silva, J.F., et al., 2005. Classical theoretical characterization of the surface plasmon absorption band for silver spherical nanoparticles suspended in water and ethylene glycol. Physica E: Low-dimension Syst. Nanostruct. 27 (1–2), 104–112.

Sung, J.H., Ji, J.H., Park, J.D., et al., 2009. Subchronic inhalation toxicity of silver nanoparticles. Toxicol. Sci. 108 (2), 452–461.

Sung, J.H., Ji, J.H., Yoon, J.U., et al., 2008. Lung function changes in Sprague-Dawley rats after prolonged inhalation exposure to silver nanoparticles. Inhal. Toxicol. 20 (6), 567–574.

Yamawaki, H., Iwai, N., 2006. Mechanisms underlying nano-sized air-pollution-mediated progression of atherosclerosis: carbon black causes cytotoxic injury/inflammation and inhibits cell growth in vascular endothelial cells. Circ. J. 70 (1), 129–140.